

New insights into the manual activities of individuals from the Phaleron cemetery (Archaic Athens, Greece)



Fotios Alexandros Karakostis ^{a,b,*}, Jane E. Buikstra ^{c,d}, Eleanna Prevedorou ^{c,d}, Elizabeth M. Hannigan ^e, Jessica Hotaling ^e, Gerhard Hotz ^f, Hannah Liedl ^g, Konstantinos Moraitis ^h, Thomas J. Siek ^d, Lukas Waltenberger ^{i,j}, Kerri J. Widrick ^d, Katerina Harvati ^{a,b}

^a Paleoanthropology, Senckenberg Centre for Human Evolution and Palaeoenvironment, Institute of Archaeological Sciences, University of Tübingen, Tübingen, 72070, Germany

^b DFG (Deutsche Forschungsgemeinschaft) Center for Advanced Studies "Words, Bones, Genes, Tools", University of Tübingen, Tübingen, 72070, Germany

^c Center for Bioarchaeological Research, School of Human Evolution and Social Change, Arizona State University, Tempe, AZ, 85281, United States

^d Malcolm H. Wiener Laboratory of Archaeological Science, American School of Classical Studies at Athens, Athens, 10676, Greece

^e Department of Anthropology, California State University, Chico, CA, 95929-0400, United States

^f Anthropological Collection, Natural History Museum of Basel, Basel, 4051, Switzerland

^g Department of Archaeology, University of Durham, Durham, United Kingdom

^h Department of Forensic Medicine and Toxicology, School of Medicine, National and Kapodistrian University of Athens, Athens, 11527, Greece

ⁱ Department of Evolutionary Biology, University of Vienna, Vienna, 1090, Austria

^j Institute for Oriental and European Archaeology, Austrian Academy of Sciences, Vienna, 1020, Austria

ARTICLE INFO

Keywords:

Physical activity

Hand muscle attachments

Entheses

Three-dimensional multivariate analysis

Archaic Greece

V.E.R.A. method

ABSTRACT

Until the early 5th century BC, Phaleron Bay was the main port of ancient Athens (Greece). On its shore, archaeologists have discovered one of the largest known cemeteries in ancient Greece, including a range of burial forms, simple pits, cremations, *larnaces* (clay tubs), and series of burials of male individuals who appear to have died violent deaths, referred to here as "atypical burials". Reconstructing the osteobiographies of these individuals will help create a deeper understanding of the socio-political conditions preceding the rise of Classical Athens. Here, we assess the habitual manual behavior of the people of Archaic Phaleron (ca. 7th – 6th cent. BC), relying on a new and precise three-dimensional method for reconstructing physical activity based on hand muscle attachment sites. This approach has been recently validated on laboratory animal samples as well as on recent human skeletons with a detailed level of long-term occupational documentation (i.e., the mid-19th century Basel Spitalfriedhof sample). Our Phaleron sample consists of 48 adequately preserved hand skeletons, of which 14 correspond to atypical burials. Our results identified consistent differences in habitual manual behaviors between atypical burials and the rest. The former present a distinctive power-grasping tendency in most skeletons, which was significantly less represented in the latter (p-values of <0.01 and 0.03). Based on a comparison with the uniquely documented Basel sample (45 individuals), this entheses pattern of the atypical burials was exclusively found in long-term heavy manual laborers. These findings reveal an important activity difference between burials typical for the Phaleron cemetery and atypical burials, suggesting that the latter were likely involved in distinctive, strenuous manual activities. The results of this pilot study comprise an important first step towards reconstructing the identity of these human skeletal remains. Future research can further elucidate the occupational profiles of these individuals through the discovery of additional well-preserved hand skeletons and by extending our analyses to other anatomical regions.

Abbreviations: "Tübingen University Validated Entheses-based Reconstruction of Activity", V.E.R.A; *abductor pollicis brevis*, ABP; *flexor pollicis brevis*, FPB; *adductor pollicis*, ADP; *extensor pollicis brevis*, EPB; *opponens pollicis*, OP; *flexor pollicis longus*, FPL; principal component analysis, PCA.

* Corresponding author. Senckenberg Centre for Human Evolution and Palaeoenvironment, University of Tübingen, Rümelinstrasse 23, Tübingen, 72070, Germany.

E-mail address: fotios-alexandros.karakostis@uni-tuebingen.de (F.A. Karakostis).

<https://doi.org/10.1016/j.jas.2021.105415>

Received 2 February 2021; Received in revised form 15 May 2021; Accepted 18 May 2021

Available online 2 June 2021

0305-4403/© 2021 Elsevier Ltd. All rights reserved.

1. Introduction

Phaleron (Palaio Faliro) lies on a bay of the Saronic Gulf, situated about four km southwest of the Acropolis of the city of Athens, Greece. During most of the Archaic period (700–480 BCE), it served as the main port of the city-state of Athens (Osborne, 2009), until it was displaced to Piraeus in the early 5th century BC (Camp, 2001; Edwards et al., 1970). Recent excavations in the port area, during the construction of the Stavros Niarchos Foundation Cultural Center, produced over 1000 burials, excavated between 2012 and 2017 (Ingvarsson-Sundström and Backstrom, 2019; Prevedorou and Buikstra, 2019; Chrysoulaki, 2020). The remains excavated during 2012–2013 anchor this study. The presence of individuals in unusual burial postures, some apparently restrained by shackles or cord bindings, intermixed with typical burials along with a lack of grave embellishments and funerary monuments, has led to emphasis upon the non-elite status of those interred in the Phaleron cemetery (Ingvarsson-Sundström and Backstrom, 2019; Chrysoulaki, 2020). The lack of grave accoutrements contrasts with the elaborations present at cemeteries, such as the Kerameikos in Athens (Lagia, 2000).

To date, more than 1700 skeletons have been excavated in Phaleron, arranged either in mass or individual burials (Ingvarsson-Sundström and Backstrom, 2019; Prevedorou and Buikstra, 2019). The majority of these involves simple pit graves, followed by pot burials, cremations with funeral pyres, stone-lined cist graves, larnakes as well as a few less usual cases (e.g., a few tile graves or a wooden boat used as a coffin) (Ingvarsson-Sundström and Backstrom, 2019). Conspicuous among this variety of burial features are a variety of “atypical” burials, so-called because they present evidence for captivity and execution (e.g., shackled or otherwise restrained individuals) and unusual burial treatments (e.g., prone or with feet & hands bound together) (Ingvarsson-Sundström and Backstrom, 2019). These “atypical” burials, recovered from pits, are those termed “biaiothanatoi” by Ingvarsson-Sundström and Backstrom (2019) and by Chrysoulaki (2020), who attribute them to a violent death. Similar burials, including apparent examples of crucified individuals, had been excavated at Phaleron early in the 20th century (Keramopoulos, 1923; Pelekidis, 1916).

The “Phaleron Bioarchaeological Project” (PBP) of the Malcolm H. Wiener Laboratory of the American School of Classical Studies at Athens (ASCSA) holds the permit for conservation and study of the remains excavated during 2012 and 2013. The PBP is constructing an osteobiography for each individual interred at the site, then making comparisons across the site, grouping burial contexts by location and by type. In this example, we will compare “typical” burials to those buried atypically individually or in smaller groups. We focus here upon the occupational manual activities of these individuals and groups.

In the absence of textual information, we must rely on skeletal information to reconstruct activities related to occupational specialization. There are several anthropological methods proposed for reconstructing habitual physical activity based on human skeletal remains (Larsen, 1999; Pearson and Lieberman, 2004). One of the most frequent avenues focuses on bony changes occurring in the areas where muscles attach (i.e., “enthesis”) (Foster et al., 2014; Henderson et al., 2017; Schrader, 2019). Several approaches to analyzing entheses have been proposed, the majority of which relies on detailed protocols for visual evaluation of enthesal robusticity and/or potential enthesopathies (Henderson et al., 2017; Mariotti et al., 2004, 2007; Villotte, 2006; Villotte et al., 2010; Villotte and Knüsel, 2013), often providing crucial insights into past human lifeways (e.g., Havelková et al., 2011; Villotte et al., 2010; Villotte and Knüsel, 2014). Other analytical approaches have focused on the three-dimensional (3D) form of entheses, relying on quantitative analyses of their 3D size and/or shape (e.g., Karakostis et al., 2018a; 2017; Karakostis and Lorenzo, 2016; Noldner and Edgar, 2013; Nolte and Wilczak, 2013; Williams-Hatala et al., 2016). However, the overall reliability of most previous approaches

using entheses to reconstruct activity in the past have often been questioned (e.g., Foster et al., 2014). In particular, previous studies have highlighted the low intra- and inter-observer repeatability of most visual scoring systems that focus explicitly on enthesal robusticity (Davis et al., 2013; Jorgensen et al., 2020; Wilczak et al., 2016), a reported lack of association between entheses and cross-sectional morphology (which is widely used for reconstructions of activity) (e.g., Michopoulou et al., 2017; Nikita et al., 2019), an absence of association between the size of a muscle and enthesal raw dimensions (Williams-Hatala et al., 2016; but see also the results of Bucchi et al., 2019; Deymier-Black et al., 2015; Karakostis et al., 2019a), as well as a broader lack of experimental validation (Wallace et al., 2017; Zumwalt, 2006).

To address these concerns, some of us have recently put forth a new and repeatable approach for reconstructing activity using muscle attachment sites (Karakostis and Harvati, 2021; Karakostis and Lorenzo, 2016), which is the first to be validated based on two laboratory animal samples (Karakostis et al., 2019a, 2019b) as well as on human skeletons with a unique level of life-long and detailed occupational documentation (Karakostis et al., 2017). In contrast to previous methods, this approach relies on a precise protocol for 3D quantification of enthesal surface areas, followed by the identification of correlations among different entheses that reflect standard muscle synergy groups (e.g., for power- or precision-grasping hand movements) (Karakostis et al., 2017, 2019a; Karakostis and Lorenzo, 2016). To date, except for our experimental studies on laboratory animal species, our research has mainly focused on muscle attachment sites of the human hand, mainly due to its fundamental role in most daily human activities (for biomechanical arguments, see Karakostis et al., 2019c). Recently, the application of this novel approach on paleoanthropological and bioarchaeological contexts has provided important insights into the habitual manual behavior of Neanderthals as well as modern humans from various geo-chronological contexts, establishing original and meaningful connections between biological and cultural lines of evidence (e.g., Karakostis et al., 2020; Karakostis et al., 2018; Karakostis and Lorenzo, 2016). In a recently published review (Karakostis and Harvati, 2021), this new approach has been named the “Tübingen University Validated Entheses-based Reconstruction of Activity” (V.E.R.A.) method.

The aim of this study is to reconstruct patterns of manual physical activity of the people of Phaleron, comparing those from “typical” burials to the atypical ones. For this purpose, we apply the above described experimentally validated methodology (i.e., the V.E.R.A. protocols) on two groups of well-preserved hand skeletons, (1) the “typical burials” from across the cemetery, and (2) the “atypical burials”, which have been defined as “biaiothanatoi” (Ingvarsson-Sundström and Backstrom, 2019; Chrysoulaki, 2020). Furthermore, we compare the hand enthesal patterns of these skeletons with those of a reference sample with uniquely detailed and lifelong occupational documentation (i.e., the mid-19th century Basel Spitalfriedhof sample; see Hotz and Steinke, 2012; Karakostis et al., 2017). Our resulting observations provide new insights into the manual activity patterns of these individuals, setting the base for further inter-disciplinary research.

2. Materials and Methods

2.1. Sampling strategy

In this pilot study, our sample of atypical burials consists of 14 adequately preserved hand skeletons, including bone elements from both anatomical sides. Their basic anthropological analysis indicated that they were all probable or possible males, which will be considered “male” for the remainder of this report. This assessment relies on the standards described in Buikstra and Ubelaker (1994). Particularly, biological sex was estimated based on morphological traits of the pelvis and the skull. Regarding the pelvis, we relied on the criteria proposed by Phenice (1969) and revised by Klales et al. (2012), involving the visual

evaluation of the ventral arc, subpubic concavity, and ischio-pubic ramus. We additionally recorded the greater sciatic notch of the ilium, following Walker (2005; after Buikstra and Ubelaker, 1994). Even though estimations relying on the greater sciatic notch are less reliable than the ones based on the pubic bones, the greater sciatic notch was more frequently preserved in the Phaleron individuals. Sex determination based on the skull relied on the widely used criteria proposed by Walker (2008; after Buikstra and Ubelaker, 1994). Overall, when the pubic bone was available, its dimorphic markers were privileged due to their verified accuracy (Kiales et al., 2012).

Biological age was assessed based on morphological changes in the os coxa (i.e., the pubic symphysis and the auricular surface), epiphyseal union (occurring in early adulthood), and the degree of cranial suture closure. Degenerative changes at the surface of the pubic symphysis were evaluated based on the Hartnett-Fulginiti revision (Hartnett, 2010) of the Suchey-Brooks method (Brooks and Suchey, 1990), whose improved accuracy and precision have been demonstrated (Merritt, 2015). In this study, we estimated age based on multiple skeletal indicators, relying on a transition analysis that involved the pubic symphysis, auricular surface, and cranial sutures. This procedure led to the calculation of a maximum likelihood estimate and a 95% confidence interval of age for each individual (Milner and Boldsen, 2016). It should be noted that, in cases of inconsistent estimates among indicators, or when a single indicator provided a more precise age estimate, the pubic symphysis was favored due to its demonstrated reliability (Merritt, 2015). For estimating the final age of young adults, epiphyseal union was privileged, whereas cranial suture closure was only used when the other indicators were not preserved. In the present study, the hand bones of all individuals presented fused epiphyses. Due to preservation issues, a relatively narrow age-range could be estimated only for six of the atypical burials, including four young (less than ca 35 years old) and two relatively old (over ca 55 years of age) individuals. For the rest, an estimated age range could either not be provided at all or it was too broad to be useful (see Materials and Methods). It should be highlighted that future research would greatly benefit from the potential analysis of additionally discovered well-preserved hand skeletons from the Phaleron cemetery (for example, those excavated in later years; see Ingvarsson-Sundström and Backstrom, 2019; Chrysoulaki, 2020; Prevedorou and Buikstra, 2019).

Our general, typical burial sample involves 34 individual skeletons, which were discovered in 29 pit graves, four cist (or cist-like) graves, and a jar burial. This sample was composed of 11 probable or possible females, 21 probable or possible males, and two cases of undetermined sex. We will simply report these as "males" and "females" and "indeterminate" for the remainder of this research paper. A relatively narrow age-range could be determined for 15 young (below ca 35 years old), six relatively older (above ca 35 years old), and two late subadult (or possibly young adult) individuals.

Our comparative analysis also includes a sample of 45 extensively documented individuals from the historical Basel-Spitalfriedhof collection (Natural History Museum in Basel, Switzerland), who lived in the broader region of the city of Basel during the mid-19th century (Hotz and Steinke, 2012; Karakostis et al., 2017). These were all adult males of low to middle socioeconomic status, between 18 and 48 years of age, whose hands presented no pathological conditions. Based on their genealogical records, none of these individuals were directly related to one another (Hotz and Steinke, 2012; Karakostis et al., 2017). Our past research has often relied on this modern comparative sample due to its unique level of occupational documentation for each person. In particular, the archives describe each individual's occupation, duration of each job, exact position at work, and hiring institution or company. Moreover, there is information on the individuals' genealogical relations, official medical records, as well as socioeconomic characteristics (Hotz and Steinke, 2012; Karakostis et al., 2017). Based on this longitudinal documentation, 23 of the sampled individuals were involved in heavy manual labor (i.e., mainly long-term construction workers of

different outdoor specialties), whereas the other 22 spent their lives performing finer and/or semi-mechanized tasks (e.g., full-time tailors and painters) (Karakostis et al., 2017). A previous application of our 3D multivariate methodology on this reference sample identified clear differences between lifelong heavy manual laborers (showing a distinctive power-grasping enthesal pattern) and long-term precision workers of lower intensity (exhibiting a consistent precision-grasping enthesal pattern involving a coordination between the thumb and index finger muscles) (Karakostis et al., 2017). In more recent research, the thorough documentation provided by this comparative sample helped our approach to interpret the grasping differences observed in unidentified bioarchaeological samples, including relatively recent case-studies (e.g., Hotz, 2017), a late medieval population from Burgos (Karakostis and Lorenzo, 2016), as well as prehistoric hunter-gatherers from diverse geo-chronological contexts (Karakostis et al., 2018b, 2020).

Following the results of our previous studies (Karakostis et al., 2017, 2018b, 2020; Karakostis and Lorenzo, 2016), we initially focused on nine hand muscle attachment sites. However, given the underrepresentation of certain bone elements in the Phaleron sample, our study relied on a total of five entheses, corresponding to six thumb muscles with central importance in human hand biomechanics (Clarkson, 2000; Karakostis et al., 2017; Karakostis and Lorenzo, 2016; Marzke et al., 1998). These involve the common attachment area of muscles *abductor pollicis brevis* and *flexor pollicis brevis* (ABP/FPB) as well as the insertion sites of muscles *opponens pollicis* (OP), *adductor pollicis brevis* (ADP), *extensor pollicis brevis* (EPB), and *flexor pollicis longus* (FPL). The general characteristics of these muscles and entheses (including the bones on which they are located) are summarized in Table 1. It is worth noting that these enthesal surfaces did not seem to present distinguishable pathological alterations in the individuals of our sample.

2.2. Precise 3D measurement of muscle attachment sites

The 3D surface of all hand bones was reconstructed using a handheld Artec Space Spider scanner (Artec Inc., Luxembourg). This equipment relies on structured-light technology, providing scans with a measuring accuracy of 50 μm . The developed 3D models were exported in PLY format and imported into the software Meshlab (Meshlab Inc., Rome) for further surface processing and analysis.

For delineating the exact borders of entheses on the bone surface, we employed the detailed protocols of the V.E.R.A. approach, whose intra- and inter-observer repeatability has been verified in previous research on the same hand muscle attachment sites (maximum mean error was 0.62%; see Karakostis and Lorenzo, 2016). In more recent work, the exact steps of this protocol were described in greater detail, including illustrations of all steps in Karakostis and Harvati (2021) (for

Table 1

The anatomical location of the five muscle attachment sites used, their abbreviation, and the function of their six associated muscles.

Muscles	Abbreviation	Main action	Analyzed attachment site
<i>Abductor pollicis</i>	ABP	Abducts the thumb	Radial base of the first proximal phalanx
<i>Flexor pollicis brevis</i>	FPB	Flexes the first metacarpophalangeal joint	(same enthesal area for both muscles)
<i>Adductor pollicis</i>	ADP	Adducts the thumb	Ulnar base of the first proximal phalanx
<i>Extensor pollicis brevis</i>	EPB	Extends the thumb	Dorsal base of the first proximal phalanx
<i>Opponens pollicis</i>	OP	Abducts, rotates, and flexes the thumb	Radial diaphysis of the first metacarpal
<i>Flexor pollicis longus</i>	FPL	Flexes the first distal phalanx	Palmar diaphysis of the first distal phalanx

experimental animal studies, also see [Karakostis et al., 2019](#)). In brief, enthesal borders are virtually defined on the bone meshes based on the criteria of surface elevation, irregularity, and coloration. The most defining criterion is surface elevation (i.e., the presence of projecting or depressing bone area). This process is greatly facilitated by various 3D imaging filters, which are available in the open-access software Meshlab. Initially, the broader enthesal area is identified on the bone using standard surface curvature algorithms (such as the filter “Discrete curvatures”). Then, the observer selects a region of the bone that encompasses both the distinctive attachment site as well as a thin zone of relatively flatter surface around the attachment site. Subsequently, applying additional filters exclusively on that bone region (i.e., “Curvature principal directions”, “Distance from borders”, or “Calculation of geodesic distances”) helps identifying the exact borders of entheses on the bone surface and allows for a direct quantification of their 3D surface areas (in mm²).

2.3. Statistical analyses

Following the V.E.R.A. protocols, the calculated 3D surface areas of all five entheses (in mm²) were used as variables in a series of principal component analyses (PCAs). These relied on a correlation matrix because the variables presented varying scales ([Table 2](#)). For all PCAs, the variables of our dataset met the assumptions for a PCA ([Field, 2013](#)), including minimum sample size requirements (i.e., a minimum of five cases per variable), approximately normal distribution (based on normal probability plots), sphericity (based on Bartlett's tests), linearity among variables (based on bivariate plots), and no outliers (according to the z-scores technique). The number of the principal components (PCs) plotted for each PCA was decided based on the standard scree-plot approach ([Cattell, 1966](#); [Field, 2013](#)). All statistical analyses of this study were carried out in the software IBM SPSS (IBM inc., Armonk, NY; version 24 for Windows). No PCA conducted in this study assumed prior group assumptions for the individuals (i.e., in the plots, cases were simply colored by group after the analysis).

A separate analysis was conducted for each anatomical side. The resulting multivariate patterns were generally symmetrical (see [Table 3](#) and figures in Results). It should be noted, however, that the PCA based on five entheses (see below) could not be performed for the left anatomical side since only one atypical burial presented all five left muscle attachment sites. To maximize sample representation, we additionally performed a mixed sides analysis that combined an individual's

left and right entheses. The best-preserved side (left or right) was defined based on the number of healthy entheses present. When an enthesis was missing from that side, this was taken from the less-preserved side, allowing the specimen to participate in the PCA. In the few cases of perfectly equal preservation between the two sides, the right side was preferred since the right entheses were overall much better preserved both in the Phaleron as well as the Basel samples. Considering that the observed patterns among groups were highly consistent between the combined sides PCA analyses ([Figs. 1–4; Table 3](#)) and those relying on each side separately ([Figs. 2, 3 and 5 to 7](#); also see PCA statistics in [Table 3](#)), our subsequent statistical comparisons focused on the combined PCAs.

Furthermore, following previous applications of our approach ([Karakostis et al., 2018b](#)), two different PCAs were run for each side separately as well as the combined dataset. The first PCA attempted to further maximize the sample size of our analysis by relying on three entheses that correspond to four thumb muscles that play a central role in hand biomechanics. These entheses correspond to four muscles inserting into the 1st proximal phalanx ([Table 1](#)): ABP/FPB, ADP, and EPB. Our previous research on these three muscle attachment sites showed that they could provide a considerable separation between lifelong occupational tendencies ([Karakostis et al., 2017, 2018b](#)). The second PCA attempted to maximize the number of enthesal variables, relying on all five muscle attachment sites, thus also considering the important contribution of muscles OP and FPL ([Table 1](#)). Both PCAs identified a principal axis of variation explaining differences between power- and precision-grasping enthesal patterns (e.g., see [Karakostis et al., 2017, 2018](#)).

We further evaluated the observed differences between atypical and typical burials using the two-sample Kolmogorov-Smirnov Z test ([Corder and Foreman, 2014](#)), a non-parametric analysis that has been recommended for comparing groups with small sample sizes ([Field, 2013](#)). We focused on the scores of selective PCs that exhibited distinctive variation between the two burial groups (see Results and figures). Furthermore, for the scores of PC2 (from the second PCA) that presented inter-population variation, we also tested for significant differences between all Phaleron and all Basel individuals. In order to control for the probability of increased Type 1 error (due to the three comparisons performed), we confirmed that p-values were still significant after adjusting them based on the Holm-Bonferroni sequential technique ([Holm, 1979](#)). Additionally, the same comparisons were applied for the raw 3D surface size (in mm²) of each of the five entheses analyzed in this

Table 2

Descriptive statistics for each variable (i.e., 3D surface area measurements for each enthesis, in mm²) per Phaleron burial group and anatomical side, including sample size (N), mean, and standard deviation (SD). Muscle abbreviations are provided in [Table 1](#). Each variable's sample size (N) does not correspond to the number of individuals used in the PCAs ([Figs. 1–7; Table 3](#)), which require the use of individual hand skeletons with all necessary entheses preserved (i.e., all first three entheses for the first PCA and all five entheses for the second PCA).

Anatomical side	Muscle attachment site	Atypical burials		Typical burials	
		N	Mean ± SD	N	Mean ± SD
Combined sides	ABP/FPB	14	76.88 ± 26.72	35	62.98 ± 16.83
	ADP	14	58.33 ± 18.48	35	50.05 ± 14.31
	EPB	14	66.74 ± 22.16	34	43.28 ± 17.06
	OP	11	90.09 ± 24.76	33	78.61 ± 19.24
	FPL	11	38.29 ± 8.78	22	30.06 ± 10.97
Right	ABP/FPB	11	81.06 ± 23.40	27	60.86 ± 16.28
	ADP	11	60.18 ± 18.65	26	49.47 ± 13.85
	EPB	10	68.87 ± 26.17	24	42.49 ± 15.33
	OP	12	83.15 ± 28.04	27	77.61 ± 19.93
	FPL	8	38.87 ± 7.63	20	31.24 ± 11.39
Left	ABP/FPB	9	73.69 ± 21.87	31	59.52 ± 15.49
	ADP	9	61.54 ± 17.12	32	50.39 ± 13.21
	EPB	8	65.94 ± 14.16	28	41.18 ± 18.21
	OP	6	71.69 ± 23.36	30	70.71 ± 19.54
	FPL	8	34.18 ± 8.15	14	27.61 ± 8.83

Table 3

Statistics of the principal component analyses performed, either on three (first PCA) or five muscle attachment sites (second PCA). Muscle abbreviations are provided in Table 1.

Analyses	Eigenvalue	Variance explained (%)	Factor loadings				
			ABP/FPB	ADP	EPB	OP	FPL
Combined sides First PCA	—	—					
PC1	2.03	67.66	0.90	0.85	0.71		
PC2	0.68	22.61	-0.19	-0.39	0.70		
Total		90.28					
Combined sides Second PCA	—	—					
PC1	2.71	54.18	0.92	0.82	0.63	0.45	0.77
PC2	0.99	19.83	0.13	-0.11	-0.16	0.87	-0.42
PC3	0.70	14.02	-0.14	-0.29	0.75	0.04	-0.17
Total		88.03					
Right side							
First PCA	—	—					
PC1	1.94	64.66	0.86	0.81	0.74		
PC2	0.65	21.69	-0.14	-0.45	0.65		
Total		86.35					
Right side							
Second PCA	—	—					
PC1	2.61	52.17	0.87	0.75	0.65	0.47	0.81
PC2	0.97	19.42	0.19	-0.25	-0.17	0.86	-0.33
PC3	0.71	14.24	-0.14	-0.41	0.72	0.03	-0.07
Total		85.82					
Left side							
First PCA	—	—					
PC1	1.98	65.92	0.86	0.86	0.71		
PC2	0.67	22.29	-0.29	-0.29	0.71		
Total		88.21					

study.

Finally, to account for the potential effects of biological age and body size on the observed multivariate patterns (PC scores), we assessed the strength of their association with biological age and estimated stature using the Spearman's correlation coefficient (r_s). Given that an exact age-group (i.e., young, middle aged, or old) and approximate stature could not be reliably indicated for most of our sample's 14 atypical burials, these statistical tests were applied only on the values of our documented reference sample from Basel (see in Karakostis et al., 2017). Nevertheless, we also provide general remarks regarding the potential effects of age on the PCA results for the Phaleron samples (see Results), focusing on the individuals for which an approximate estimation of age-group was available.

3. Results

The basic characteristics of this study's variables are provided for each anatomical side in Table 2. All PCA statistics (eigenvalues, percentages of variance, and factor loadings) are presented in Table 3. As it can be observed in Table 3 and the figures (Figs. 1–7), all the statistics and multivariate patterns described below were consistently similar between the combined-sides PCAs and the PCAs on each side separately (also see Discussion).

For the combined-sides first PCA, which was based on three enthesal variables, the scree-plot approach recommended focusing on PC1 and PC2, representing a total of 90.2% of total variance in the sample (Fig. 1). Based on the factor loadings (Table 3), PC1 (67.4% of the sample's variance) represented overall size differences across specimens (i.e., all factor loadings were positive), indicating that individuals with higher PC1 scores presented overall larger entheses. In contrast, variation on PC2 (22.8%) reflects the proportion between two entheses of three thumb thenar muscles (ABP_FPB and ADP) and the insertion site of EPB, a thumb's main extensor muscle (Table 1). Both Phaleron groups extensively overlap on PC1, despite a clear tendency of smaller enthesal size in the typical burial group (i.e., most cases show low PC scores). On PC2, our documented sample's lifelong heavy manual workers present

distinctively higher positive scores (i.e., proportionally larger EPB), whereas long-term precision workers show lower scores (i.e., proportionally larger thenar muscles associated with flexion, abduction, and adduction at the trapezio-metacarpal joint). This broadly reflects the results of our previous research for the documented Basel sample (Karakostis et al., 2017, 2018b, 2020). On this axis, 11 of the 14 atypical burials present distinctively higher scores, exclusively overlapping with lifelong heavy manual laborers, while three of them show low scores and coincide with long-term precision workers. Regarding the typical burial sample, even though its majority overlaps with heavy manual laborers, their PC2 values are consistently lower than those of the atypical burials. Moreover, several of their scores (12/34) coincide with those of long-term precision workers. It is worth noting that the males and females of this group exhibit similar PC2 values, but none of the 11 females show very high positive PC2 values (Fig. 1). Consequently, there is a distinct area in the uppermost part of the PC2 axis that includes only males, including several long-term heavy construction workers, most of the atypical burial sample (10 of 14), and three individuals from the typical burial sample.

For the combined second PCA (based on five entheses and fewer Phaleron individuals), the scree-plot recommended focusing on the first 3 PCs (representing a total of 88.0% of sample variance). As in the combined first PCA (Fig. 1), PC1 (54.2%) represents overall 3D size variation in the sample (Table 3; Figs. 2 and 3), while the factor loadings of PC3 (14.0%) are very similar to those of PC2 of the combined first PCA (the one based on three entheses). Consequently, the observed PC3 patterns are clearly equivalent, with 7 out of 9 atypical burials overlapping with heavy manual laborers and two males from the general burial sample (Fig. 4). Nevertheless, PC2 (19.8%) reveals a different pattern of variation in the sample. On this axis, the two Phaleron samples broadly overlap in the positive side of the component, while most Basel individuals present negative PC2 scores (see horizontal PC2 axis of Fig. 4). Based on this PC2's factor loadings (Table 3), Phaleron individuals consistently present a proportionally larger insertion site for OP, a muscle of central importance for thumb opposition (Table 1). On this component, there is no clear distinction between long-term heavy

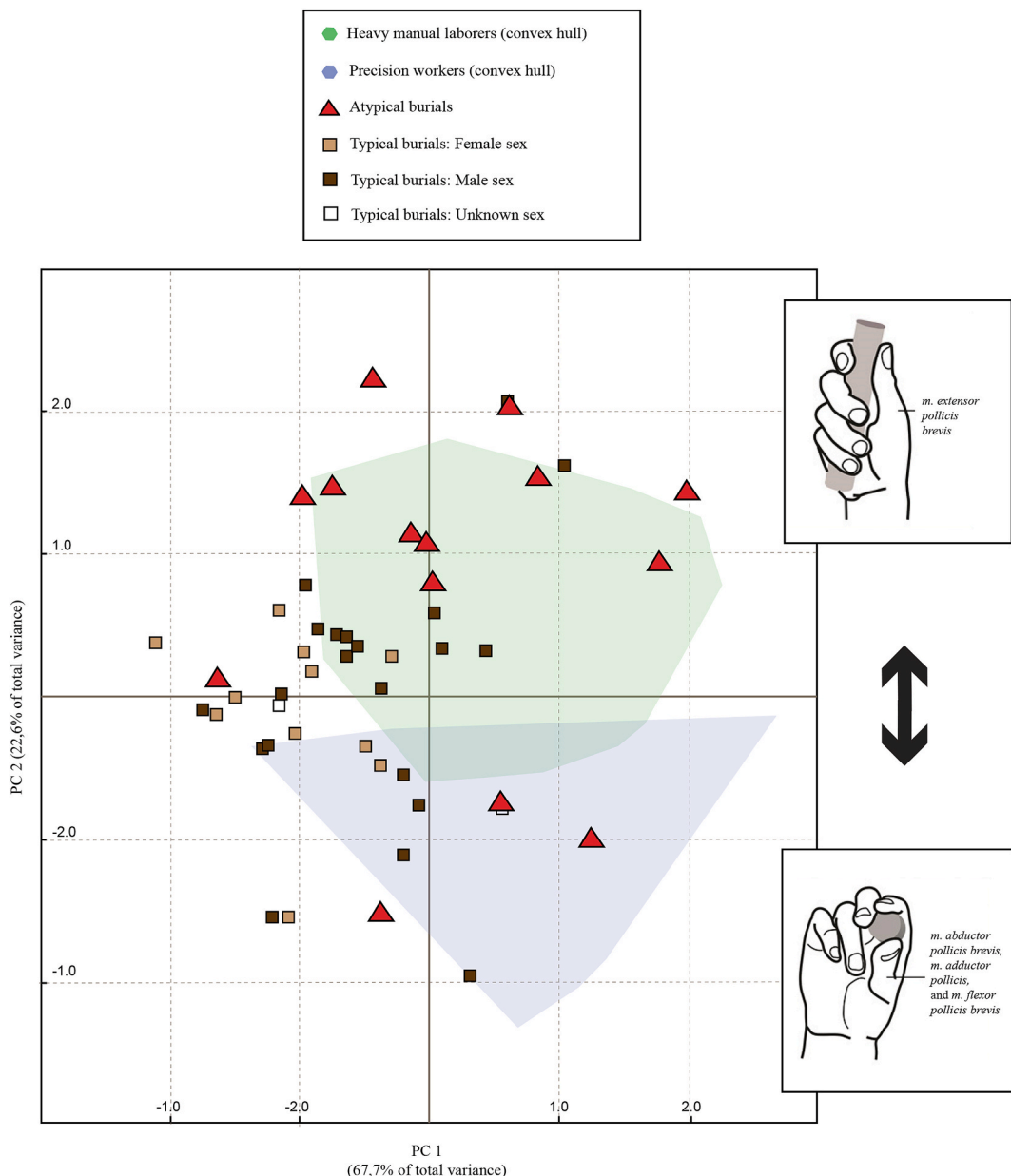


Fig. 1. Plot of the principal component analysis (PCA) based on the 3D area measurements of three muscle attachment sites and all individuals preserving these entheses. This PCA was conducted on a dataset combining entheses from both anatomical sides, after confirming that results were consistent across PCAs (see Materials and Methods). No groups were assumed *a priori*. For the purpose of visual clarity, the documented samples from Basel are only represented in the plot by their convex hulls (for an extensive description of manual enthesal patterns in the same exact individuals, see Karakostis (2017, 2018b, 2020)). The upper side illustration summarizes the main pattern presented by individuals with higher PC2 values (i.e., a proportionally larger enthesis for extensor pollicis brevis; see Table 3), while the lower side image is associated with cases with lower PC2 scores (i.e., proportionally larger attachment sites for muscles abductor pollicis brevis, flexor pollicis brevis, and adductor pollicis; see Table 3). The two side figures were modified after Karakostis et al. (2018b).

manual laborers and precision workers.

As outlined in Materials and Methods, the main enthesal patterns observed for the combined-sides dataset were also consistently present in the analyses focusing on each anatomical side separately (see factor loadings for all PCAs in Table 3). The latter include the two PCAs involving entheses of the right hand (Figs. 5 and 6; also see PC1 scores in Figs. 2 and 3) as well as the PCA on three left enthesal measurements (Fig. 7).

The results of the two-sample Kolmogorov-Smirnov Z tests further supported the above observations of enthesal differences between burial groups (Table 4). A statistically significant difference was found between typical and atypical burials in the scores of both PC2 (in the first PCA; Fig. 1) and PC3 (in the second PCA; Fig. 4). Furthermore, a

significant difference was also found between all Phaleron and all Basel individuals in the PC2 values of the second PCA (Fig. 4). In raw 3D size, EPB showed a significant difference between burial groups, while four of the five entheses significantly varied between Basel and Phaleron (Table 5).

The results of the correlation tests on our documented reference sample confirmed that the multivariate patterns observed in the PCAs (Figs. 1 and 4) were not significantly associated with interindividual variation in biological age or stature. Biological age and predicted stature were not correlated with the PCs that represented variation in proportions among different entheses (i.e., PC2 of the first PCA, PC2 of the second PCA, and PC3 of the second PCA), with p-values ranging between 0.12 and 0.74. In contrast, in agreement with previous studies

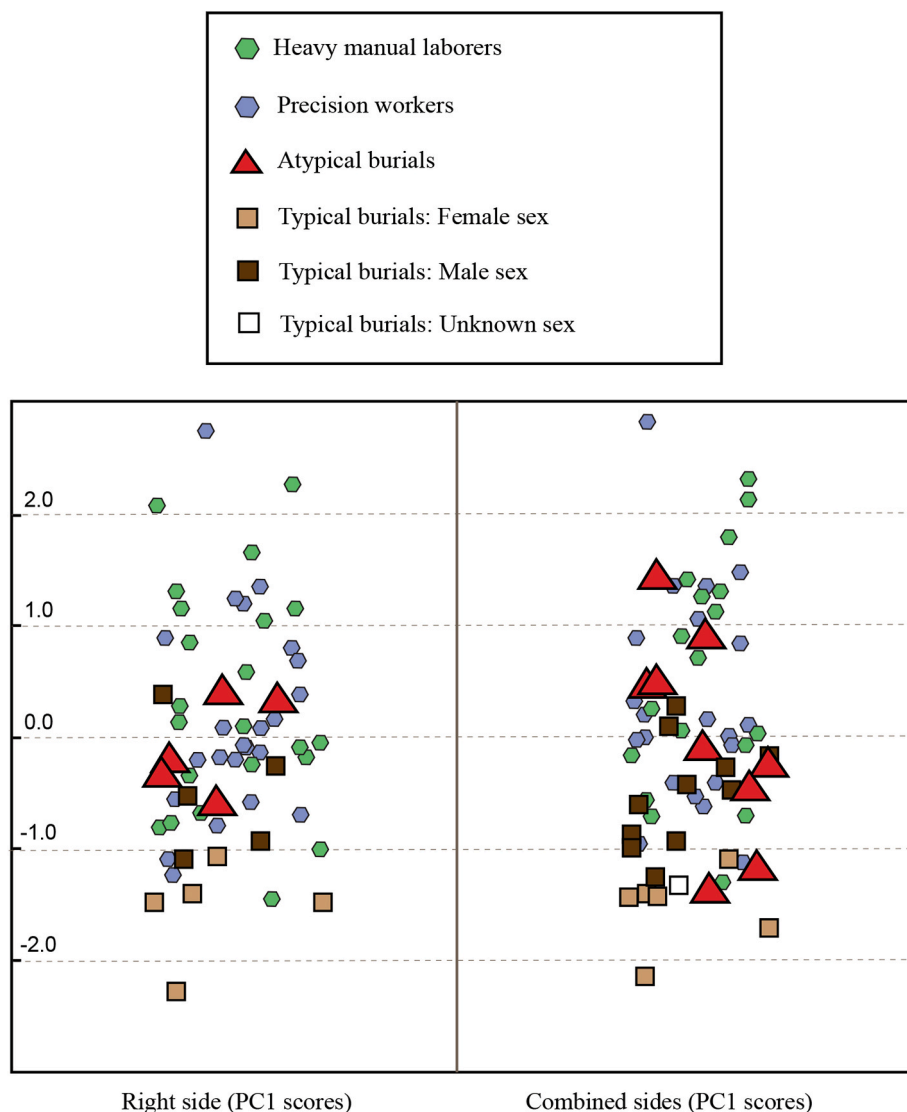


Fig. 2. Jitter plots presenting the principal component 1 (PC1) scores of the two principal component analyses based on five muscle attachment sites (i.e., the one on combined anatomical sides and the one only on the right hand entheses). Based on the factor loadings (Table 3), interindividual variation on each of these components represents differences in overall enthesal size (i.e., higher scores represent overall larger sets of muscle attachment areas).

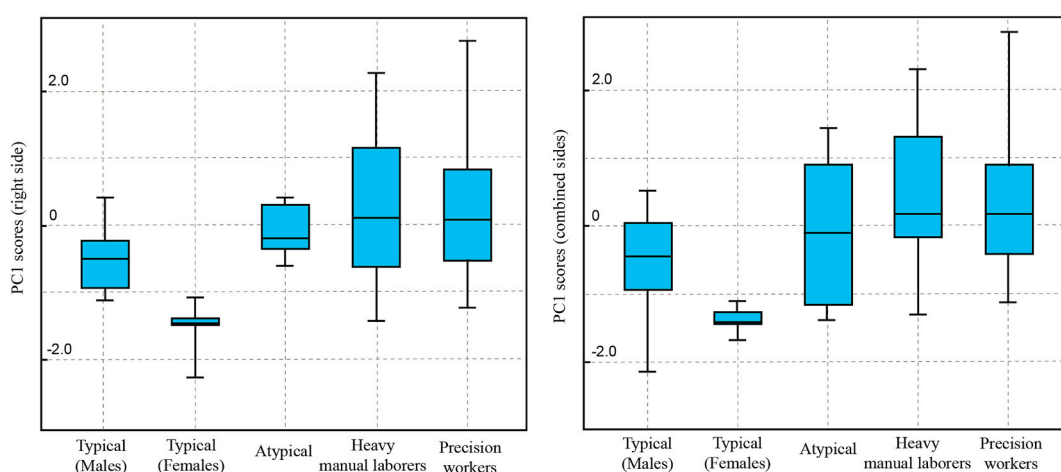


Fig. 3. Boxplots presenting the principal component 1 (PC1) scores of the two principal component analyses based on five muscle attachment sites (i.e., the one on combined anatomical sides and the one only on the right hand entheses). Based on the factor loadings (Table 3), interindividual variation on each of these components represents differences in overall enthesal size (i.e., higher scores represent larger sets of muscle attachment areas).

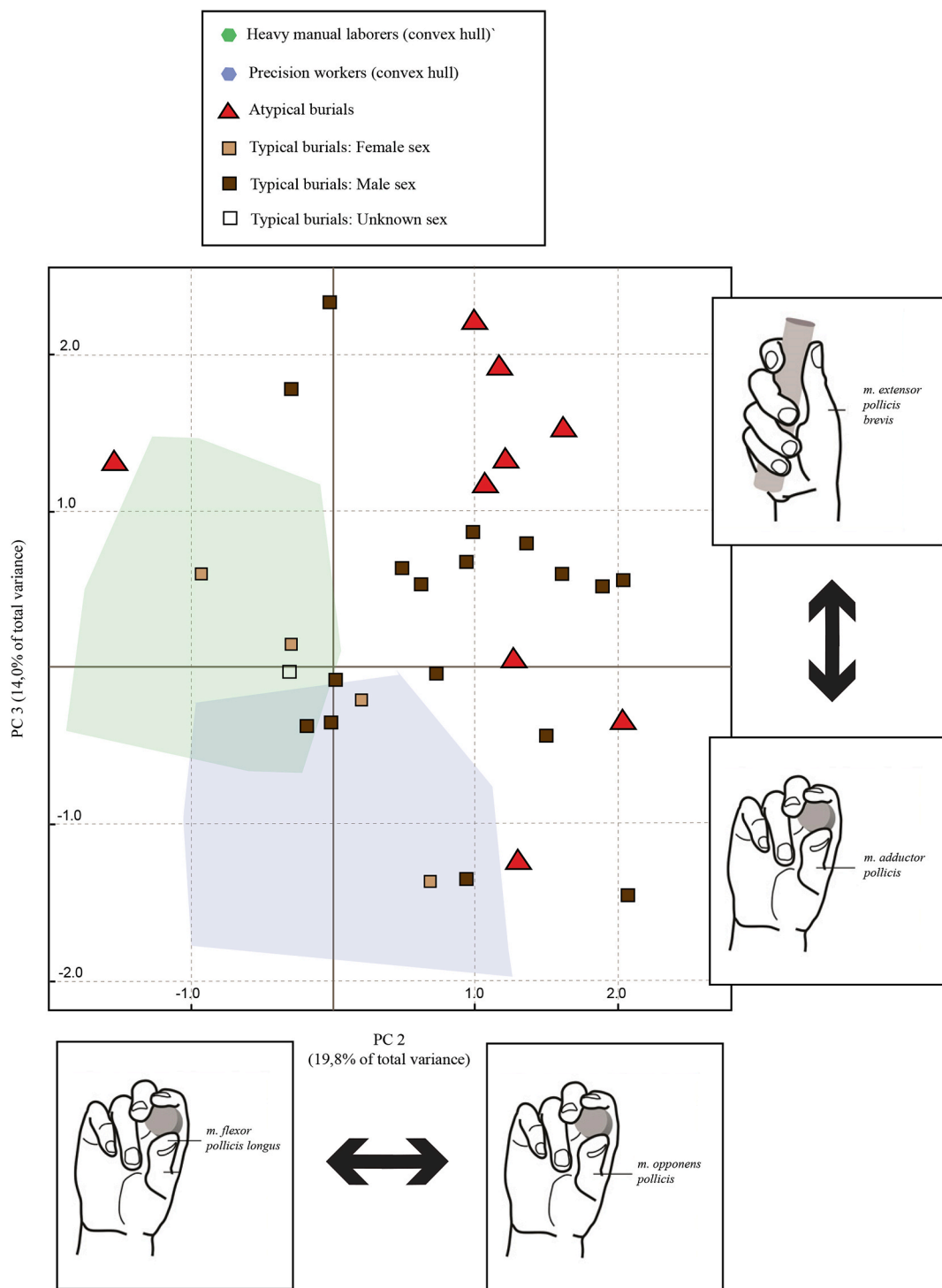


Fig. 4. Plot of the principal component analysis (PCA2 and PC3) based on the 3D area measurements of five muscle attachment sites and all individuals preserving these entheses. This PCA was conducted on a dataset combining entheses from both anatomical sides, after confirming that results were consistent across PCAs (see Materials and Methods). No groups were assumed *a priori*. For the purpose of visual clarity, the documented samples from Basel are only represented in the plot by their convex hulls (for an extensive description of manual enthesal patterns in the same exact individuals, see Karakostis (2017, 2018b, 2020). Reflecting the vertical axis of the previous PCA (Fig. 1), the top illustration summarizes the main pattern presented by individuals with higher PC3 scores, while the bottom image is associated with cases with lower PC3 scores. Respectively, the side illustrations summarize the main enthesal patterns of individuals with lower (left) and higher (right) PC2 values (see Table 3). Variation on PC2 represents the proportional enthesal size of muscle *opponens pollicis*. The four side figures were modified after Karakostis et al. (2018b).

(Karakostis et al., 2017; Karakostis and Lorenzo, 2016), the components representing overall size variation (i.e., PC1 in both PCAs) were significantly and positively correlated with biological age (p-value: 0.01; r_s : 0.46 and 0.47, respectively) and predicted stature (p-value < 0.01; r_s :

0.55, in both cases). This indicates a positive association between the raw size of entheses and the individuals' age and estimated stature, suggesting that the observed significant differences in raw 3D size (see comparisons listed in Table 5) may likely be affected by systemic factors

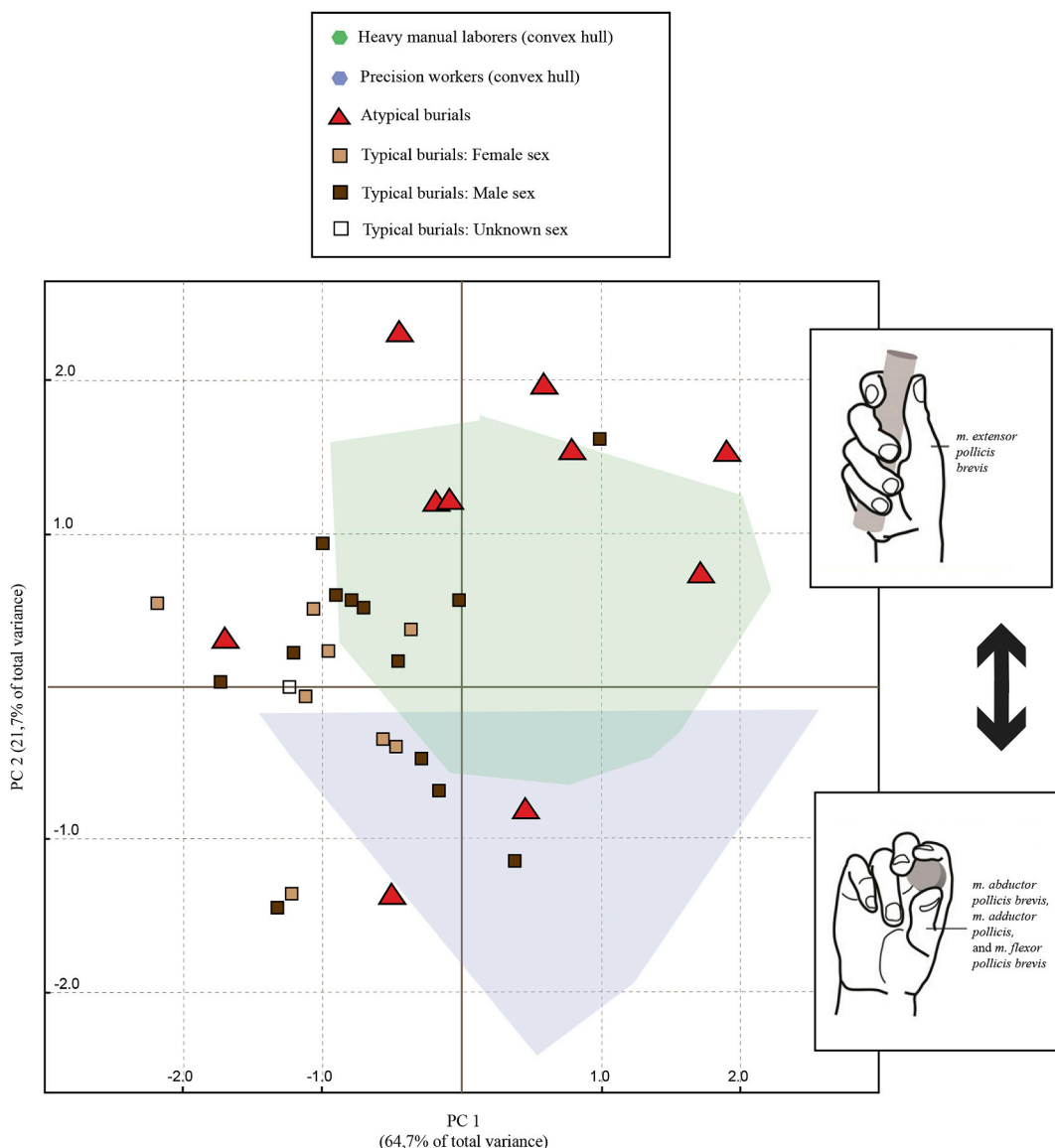


Fig. 5. Plot of the principal component analysis (PC1 and PC2) based on the 3D area measurements of three right muscle attachment sites and all individuals preserving these entheses. No groups were assumed *a priori*. For the purpose of visual clarity, the documented samples from Basel are only represented in the plot by their convex hulls (for an extensive description of manual enthesal patterns in the same exact individuals, see Karakostis et al., 2020, (Karakostis et al., 2018b), 2017). Reflecting the vertical axes of the PCAs on combined sides (Figs. 1 and 4), the top illustration summarizes the main pattern presented by individuals with higher PC2 scores, while the bottom image is associated with cases with lower PC2 values (see Table 3). The two side figures were modified after (Karakostis et al., 2018b).

of interindividual enthesal variation (as also demonstrated in previous studies; see extensive review by Karakostis and Harvati, 2021). Among the Phaleron individuals of our sample whose exact age-group could be assessed (see Materials and Methods), there was no clear distinction across age-groups within each sample. All calculated PCs for older and younger individuals appeared to broadly overlap within each burial group. Nevertheless, it should be noted that, for the atypical burial group, the two potentially older individuals (i.e., burials IV_560 and 5_198) exhibited positive PC1 scores (i.e., larger overall enthesal 3D size).

4. Discussion

The results of this study revealed a consistent power-grasping tendency in most hand skeletons of the atypical burial sample ("biaiotha-natoi"; Ingvarsson-Sundström and Backstrom, 2019; Chrysoulaki, 2020), which led them to overlap exclusively with documented

long-term heavy manual laborers (Figs. 1 and 4 to 7; also see Table 4). This tendency was present but distinctively lower in the individuals of the general burial sample, several of which exhibited precision-grasping enthesal patterns (overlapping with recent long-term precision workers). In terms of habitual manual behavior, these results suggest that most individuals of our atypical burial sample were involved in comparatively more strenuous activities than those in the general burial sample. In our recent documented sample, similar enthesal patterns were only found in long-term heavy manual laborers (mainly recent heavy construction workers, such as bricklayers, carpenters, stonemasons, etc.). However, it is crucial to clarify that this observed similarity does not indicate that the individuals of the atypical burial sample themselves were necessarily construction workers, but rather that their lifestyles likely shared a comparatively high frequency (and/or intensity) of generalized power-grasping motions. Multiple strenuous manual activities have been reported for the inhabitants of Archaic and Classical Athens, such as farming, quarrying, mining, sea-faring,

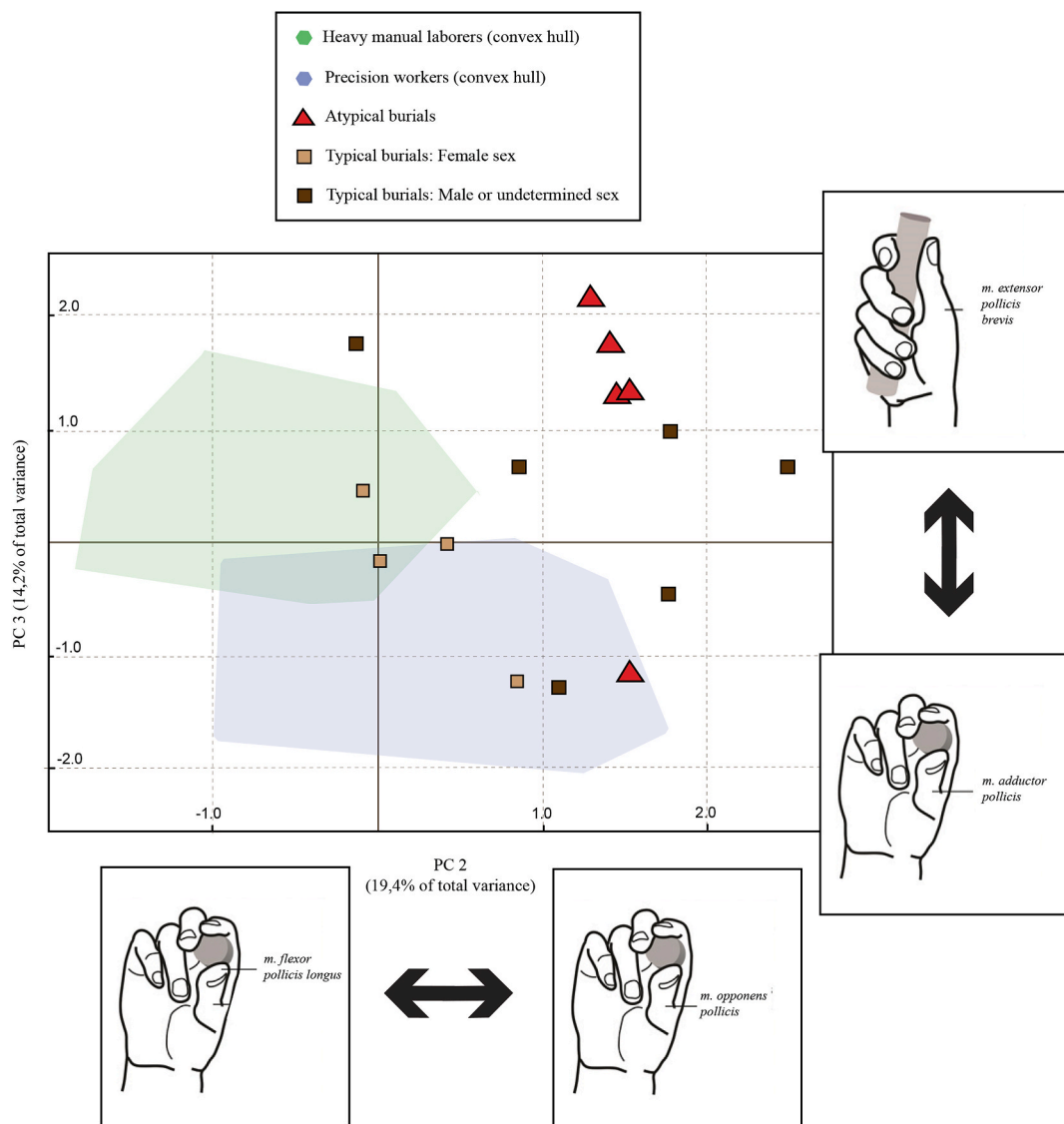


Fig. 6. Plot of the principal component analysis (PC2 and PC3) based on the 3D area measurements of five right muscle attachment sites and all individuals preserving these entheses. No groups were assumed *a priori*. For the purpose of visual clarity, the documented samples from Basel are only represented in the plot by their convex hulls (for an extensive description of manual enthesal patterns in the same exact individuals, see Karakostis et al., 2020, (Karakostis et al., 2018b), 2017). Reflecting the horizontal and vertical axes of the corresponding PCA on combined sides (Fig. 4), the two top and two side illustrations summarize the main enthesal patterns observed in each direction of the two components (see Table 3). The four side figures were modified after (Karakostis et al., 2018b).

construction building, warfare, sports, and others (Hall, 2007; Morris, 2009; Osborne, 2009). With the exception of warfare and sports, most of these tasks were typically associated with individuals of lower or middle socioeconomic status (Golden, 2009; Nicholson, 2011; Osborne, 2009; Pritchard, 2012).

It is worth noting that all individuals of our atypical burial sample seem to be of male sex (see Materials and Methods; also see Ingvarsson-Sundström and Backstrom, 2019). In all our PCAs (Figs. 1 and 4 to 7), most of them occupied the uppermost area of the plots (i.e., high scores on the vertical axes), overlapping exclusively with certain male individuals of the typical burial group. This could perhaps be indicative of behavioral differences between sexes, suggesting that some of the males (including most atypical burials) may have been involved in more strenuous manual tasks than all other males and females. However, given the limited representation of potential female skeletons in our study ($N = 11$), we believe that this possibility can only be properly addressed through future research on increased female sample sizes (in the atypical group). Additionally, considering the sexual division of labor in Archaic Athens (Hall, 2007), one could argue that incorporating

females to analyses of male-only samples (i.e., atypical burials and the Basel individuals) may have affected our results on manual activity. To ensure that this is not the case, we have re-run all analyses without the 11 females, confirming that all observed enthesal patterns (PCAs) as well as statistical test outputs (i.e., significance of two-sample Kolmogorov-Smirnov results) did not considerably alter in any way.

Due to preservation issues, it was impossible to directly assess the effects of biological age on the enthesal patterns of the Phaleron individuals. Nevertheless, our tests focusing on the comparative sample from Basel showed that only PC1, which reflected overall enthesal size (see factor loadings in Table 3), presented a strong association with age and stature. On the contrary, the other PCs (PC2 and PC3), which represented variation in proportions among different entheses, did not present such correlations in the documented individuals. This directly reflects the results of our previous research on the same mid-19th century Basel sample (Karakostis et al., 2017). In the present study, on the PC1 axis, individuals from all groups (Basel and Phaleron) extensively overlap in all analyses (e.g., see the PCA plot of Fig. 1). At the same time, numerous individuals with almost identical values on PC1 (representing

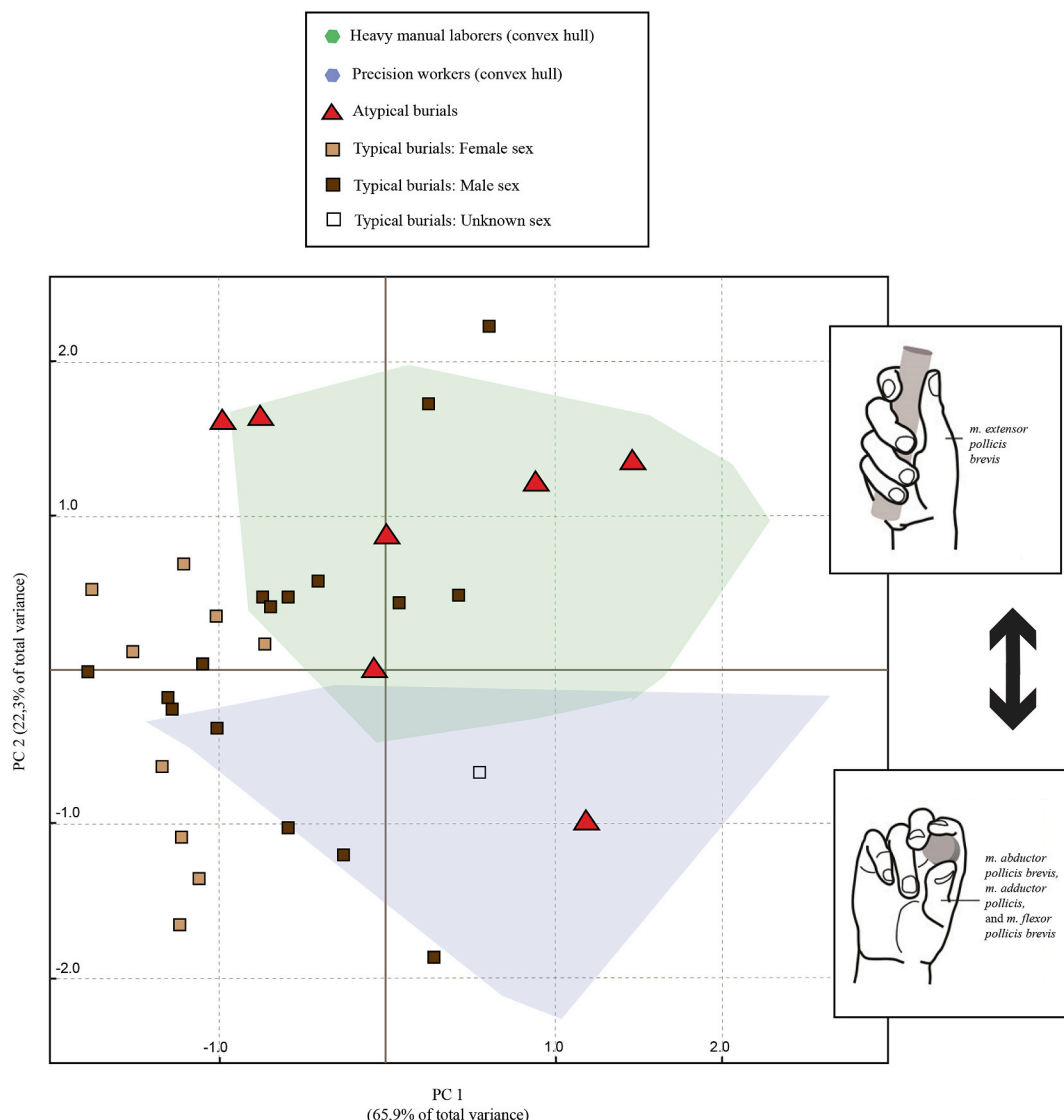


Fig. 7. Plot of the principal component analysis (PC1 and PC2) based on the 3D area measurements of three left muscle attachment sites and all individuals preserving these entheses. No groups were assumed *a priori*. For the purpose of visual clarity, the documented samples from Basel are only represented in the plot by their convex hulls (for an extensive description of manual enthesal patterns in the same exact individuals, see Karakostis et al., 2020, (Karakostis et al., 2018b), 2017). Reflecting the vertical axes of the PCAs on combined sides (Figs. 1 and 4) as well as the ones on right hand entheses (Figs. 5 and 6), the top illustration summarizes the main pattern presented by individuals with higher PC2 scores, while the bottom image is associated with cases with lower PC2 values (see Table 3). The two side figures were modified after (Karakostis et al., 2018b).

Table 4

Comparisons of multivariate patterns (PC scores) between groups using the two-sample Kolmogorov-Smirnov Z tests. All three p-values remained statistically significant (below 0.05) even after correction using the Holm-Bonferroni sequential technique (see Materials and Methods). The terms “atypical” and “typical” refer to the two Phaleron burial groups studied, while “reference sample” indicates the thoroughly documented individuals from the Basel Spitalfriedhof collection (Switzerland).

Groups compared	Variable	Z-value	P-value
Atypical	Typical	PC2 scores (first PCA)	2.06 < 0.01
Atypical	Typical	PC3 scores (second PCA)	1.46 0.03
Phaleron	Reference sample	PC2 scores (second PCA)	2.87 < 0.01

overall size) present distinctive scores on the vertical axis PC2 (representing proportions among different entheses), which is the variable demonstrating the group differences highlighted in this study. Thus, if one were to propose a major effect of biological age on the observed

differences between typical and atypical burials, it would have to be assumed that, in contrast to what is observed in other population samples (Karakostis et al., 2017; Karakostis and Lorenzo, 2016), degenerative changes did not only affect the raw size of entheses, but also impacted the proportions among different entheses of each Phaleron individual. Simultaneously, it would also have to be assumed that, especially for the atypical burials (but not the typical ones), these hypothetically age-driven proportions happened to largely coincide with the patterns of documented lifelong manual laborers from a recent sample (of varying biological ages), while also coincidentally reflecting greater thumb extension (i.e., recruitment of EPB; see Tables 1 and 3). Even though it is impossible to entirely dismiss the above scenario due to the absence of reliable age assessment for most Phaleron individuals, we do not consider it the most parsimonious interpretation of our results.

Despite the above differences between atypical and typical burial samples, the results of this study also revealed important similarities. In all PCAs, most individuals of both groups share an overall power-grasping tendency (even if that is systematically higher in most

Table 5

Comparisons of raw 3D surface measurements (in mm²) between groups using the two-sample Kolmogorov-Smirnov Z tests. P-values that remained significant after sequential correction (for each set of five comparisons; [Field, 2013](#); [Holm, 1979](#)) are in bold. The terms “atypical” and “typical” refer to the two Phaleron burial groups studied, while “reference sample” indicates the thoroughly documented individuals from the Basel Spitalfriedhof collection (Switzerland). Abbreviations of muscle/enthuses are spelled out in [Table 1](#).

Groups compared		Raw Measurement	Z-value	P-value
Atypical	Typical	OP	1.48	0.03
Atypical	Typical	ABP/FPB	1.22	0.10
Atypical	Typical	ADP	0.72	0.67
Atypical	Typical	FPL	1.35	0.05
Atypical	Typical	EPB	2.24	<0.01
Phaleron	Reference sample	OP	1.63	0.01
Phaleron	Reference sample	ABP/FPB	1.60	0.01
Phaleron	Reference sample	ADP	2.31	<0.01
Phaleron	Reference sample	FPL	4.00	<0.01
Phaleron	Reference sample	EPB	1.07	0.20

individuals of the atypical burial sample; [Figs. 1 and 4 to 7](#)). Furthermore, our analyses identified one axis of variance (i.e., PC2 of the second PCA; [Fig. 4](#)), which grouped the majority of the Phaleron individuals together in the positive side of the plot, opposite to most values of our modern documented sample from Basel. This difference between the two population samples, which was found to be statistically significant ([Table 4](#)), may likely be due to various systemic factors of interpopulation variation in enthesal morphology, such as genes, nutrition, hormones, and age ([Foster et al., 2014](#); [Schrader, 2019](#); [Villotte and Knüsel, 2013](#)). In this framework, one could argue that perhaps the unknown effects of these factors may have affected this study's interpretations (e.g., coincidentally leading to the observed overlapping between Basel's lifelong manual workers and Phaleron's atypical burials). However, the Phaleron individuals would still present the observed enthesal patterns (e.g., the one reflecting intense thumb extension in most atypical burials) even without including Basel's lifelong manual laborers in the analyses. That comparison is nevertheless essential for our study's interpretations because it confirms that, in a sample with thorough and long-term occupational documentation, such an enthesal pattern is almost exclusively found in lifelong heavy manual laborers.

Even though the methods and results of the present study cannot be used to directly assess population origin, the above enthesal similarities between the two Phaleron groups may be indicative that they both originate from a broadly similar population, at least in terms of general lifestyle and living conditions. This possibility may be also further supported by comparisons among groups in bone pathology and epigenetic traits. Future paleogenetic analysis of the Phaleron skeletons may be able to provide further insights into whether these burial groups represent different populations. Nevertheless, it is worth noting that enthesal variation in our thoroughly documented sample from Basel was not associated with familial relatedness (see [Karakostis et al., 2017](#)). Therefore, we would find it unlikely that the same exact PCs (e.g., [Fig. 1](#)) representing occupational differences in one population (Basel) would then be driven exclusively by genetic factors in the Phaleron samples.

The multivariate results of the present study were consistent between the PCAs combining anatomical sides ([Figs. 1 and 4; Table 3](#)) and those performed on each side separately ([Figs. 5–7; Table 3](#)). Previous research on our documented sample from Basel (also following the V.E. R.A. approach) had also reported similar enthesal correlations between the left and the right side of each individual (see [Karakostis et al., 2018](#)).

As discussed in that previous research, we believe that such consistency between sides is to be expected for hand enthesal multivariate patterns, regardless of hand preference. This is because a construction worker's preference for using one anatomical side does not negate the fact that heavy manual labor requires bimanual hand use. At the same time, a tailor's precise grasping in one anatomical side does not equate the habitual performance of intense power-grasping in the other. In the comparative framework of a PCA, the signal of intra-individual bilateral differences is likely weaker than the variation across individuals with distinct occupational specializations.

5. Conclusions

The aim of this study was to provide new insights into the identity of the Phaleron's atypical burials, comparing a general burial sample with a group of apparently executed individuals buried near a major port of Archaic and early Classical Athens. Our results revealed a shared component among most of the latter individuals, who presented evidence of unusually strenuous manual activities in their hand skeletal remains. Such patterns were present but significantly less distinctive in most of their surrounding burials. Despite the limited sample sizes of this pilot study, its findings comprise a crucial step in creating osteobiographies for these individuals, which will provide a deeper understanding of the socio-political conditions that preceded the rise of Classical Age Athens. We believe that future research could further elucidate the occupational and socioeconomic profiles of the Phaleron burials, hopefully relying on the potential inclusion of additional well-preserved human remains from this cemetery. For instance, extending our research to the muscle attachment sites of other important anatomical regions would likely allow for greater resolution of habitual physical activities. Such data could be further combined with other potential sources of information, involving enthesopathies, osteoarthritis, cross-sectional geometric properties of the long bones, Schmorl's nodes, dental wear, palaeogenetics, and isotopic analyses. Importantly, more nuanced hypotheses on physical activity and socioeconomic status would benefit from a deeper historical investigation of occupational differences in ancient Greece during the historical period in question.

Data availability

The data that support the findings of this study are available from the corresponding author upon reasonable request.

Declaration of competing interest

The authors declare that they have no known competing financial interests or personal relationships that could have appeared to influence the work reported in this paper.

Acknowledgements

We want to thank the excavator Dr. Stella Chrysoulaki and the Ephorate of Piraeus and Islands for the amicable collaboration. Our study and analysis of the human skeletal remains from the cemetery at Phaleron follows the permit issued by the Hellenic Ministry of Culture (ΥΠΟΠΑΙΘ/ΓΔΑΠΚ/ΔΙΠΚΑ/ΤΕΕΑΕΙ158386/93923/8033/777). We are grateful to our funding bodies: the Malcolm H. Wiener Foundation, the American School of Classical Studies at Athens, the Paul and Alexandra Canellopoulos Foundation, the School for Human Evolution and Social Change at Arizona State University, the Desnick Family, the

National Endowment for the Humanities (Collaborative Research Grant RZ-255623-17), and the National Science Foundation (Senior Archaeology Award BCS-1828645). Special thanks are due to Panagiotis Karakostis, Jim Wright, and Jenifer Neils. The authors are also very grateful to the volunteers of the “Citizen Science Project Basel Spitalfriedhof” (University of Basel, Switzerland) for their hard work on the detailed documentation of our reference sample. Finally, we would like to deeply thank Ioanna Anastopoulou and Giannis Kordonoulis for technical assistance.

References

Brooks, S., Suchey, J.M., 1990. Skeletal age determination based on the os pubis: a comparison of the Acsádi-Nemeskéri and Suchey-Brooks methods. *Hum. Evol.* 5, 227–238. <https://doi.org/10.1007/BF02437238>.

Bucchi, A., manzanares, M.C., Luengo, J., Bucchi, C., Lorenzo, C., 2019. Muscle strength and enthesal size in human thumbs: testing the relationship with a cadaveric model. *UISPP* 2, 38–42.

Buikstra, J.E., Ubelaker, D.H., 1994. Standards for Data Collection from Human Skeletal Remains. Research Series No. 44. Arkansas Archaeological Survey Research Series No 44. Fayetteville.

Camp, J.M., 2001. The Archaeology of Athens. Yale University Press, Yale.

Cattell, R.B., 1966. The scree test for the number of factors. *Multivariate Behav. Res.* 1, 245–276.

Chryssoulaki, S., 2020. The excavations at Phaleron cemetery 2012–2017: an introduction. In: Graml, C., Doronzo, A., Capozzoli, V. (Eds.), *Rethinking Athens before the Persian Wars*. Utzverlag, Munich, pp. 103–113.

Clarkson, H.M., 2000. *Musculoskeletal Assessment: Joint Range of Motion and Manual Muscle Strength*. Lippincott Williams & Wilkins, Dallas.

Corder, G.W., Foreman, D.I., 2014. *Nonparametric Statistics: A Step-by-step Approach*. John Wiley & Sons, London.

Davis, C.B., Shuler, K.A., Danforth, M.E., Herndon, K.E., 2013. Patterns of interobserver error in the scoring of enthesal changes. *Int. J. Osteoarchaeol.* 23, 147–151. <https://doi.org/10.1002/oa.2277>.

Deymier-Black, A.C., Pasteris, J.D., Genin, G.M., Thomopoulos, S., 2015. Allometry of the tendon enthesis: mechanisms of load transfer between tendon and bone. *J. Biomech. Eng.* 137, 111005. <https://doi.org/10.1115/1.4031571>.

Edwards, I.E.S., Gadd, C.J., Hammond, N.G.L., Boardman, J., Lewis, D.M., Walbank, F. W., Astin, A.E., Crook, J.A., Lintott, A.W., Rawson, E., Bowman, A.K., Champlin, E., Garnsey, P., Rathbone, D., Cameron, A., Ward-Perkins, B., Whitby, M., 1970. *The Cambridge Ancient History*. Cambridge University Press, Cambridge.

Field, A., 2013. *Discovering Statistics Using SPSS*, 4th Revised edition. SAGE Publications Ltd, California.

Foster, A., Buckley, H., Tayles, N., 2014. Using enthesis robusticity to infer activity in the past: a review. *J. Archaeol. Method Theor.* 21, 511–533. <https://doi.org/10.1007/s10816-012-9156-1>.

Golden, M., 2009. *Greek Sport and Social Status*. University of Texas Press, Texas.

Hall, J.M., 2007. *A History of the Archaic Greek World: Ca. 1200 - 479 BC*. Wiley-Blackwell, London.

Hartnett, K.M., 2010. Analysis of age-at-death estimation using data from a new, modern autopsy sample—part I: pubic bone. *J. Forensic Sci.* 55, 1145–1151. <https://doi.org/10.1111/j.1556-4029.2010.01399.x>.

Havelková, P., Villotte, S., Velemínský, P., Poláček, L., Dobisíková, M., 2011. Enthesopathies and activity patterns in the early medieval great moravian population: evidence of division of labour. *Int. J. Osteoarchaeol.* 21, 487–504. <https://doi.org/10.1002/oa.1164>.

Henderson, C.Y., Mariotti, V., Santos, F., Villotte, S., Wilczak, C.A., 2017. The new Coimbra method for recording enthesal changes and the effect of age-at-death. *B.M. S.A.P.* 29, 140–149. <https://doi.org/10.1007/s13219-017-0185-x>.

Holm, S., 1979. A simple sequentially rejective multiple test procedure. *Scand. J. Stat.* 6, 65–70.

Hotz, G., 2017. Theo der Pfeifenraucher – ein genealogisch-naturwissenschaftliches Identifizierungsprojekt. der Schweizerischen Gesellschaft für Familienforschung (SGFF) 44, 29–61.

Hotz, G., Steinke, H., 2012. Knochen, Skelette, Krankengeschichten : Spitalfriedhof und Spitalarchiv - zwei sich ergänzende Quellen. *Basl. Z. Gesch. Altertumskd.* Bd. 112, 105–138.

Ingvarsson-Sundström, A., Backstrom, Y., 2019. Bioarchaeological Field Analysis of Human Remains from the Mass Graves at Phaleron, Greece : with an Introduction by Stella Chryssoulaki and an Appendix by Anna Linderholm, Anna Kjellstrom, Vendela Kempe Lagerholm, and Maja Krzewiriska. Swedish Institute of Athens and Rome, Stockholm.

Jorgensen, K.C., Mallon, L., Kranioti, E.F., 2020. Testing interobserver and intraobserver agreement of the original and revised Coimbra Methods. *Int. J. Osteoarchaeol.* 30, 769–777. <https://doi.org/10.1002/oa.2907>.

Karakostis, F.A., Harvati, K., 2021. New horizons in reconstructing past human behavior: introducing the “tübingen university validated entheses-based reconstruction of activity” method. *Evol. Anthropol.* <https://doi.org/10.1002/evan.21892>.

Karakostis, F.A., Hotz, G., Scherf, H., Wahl, J., Harvati, K., 2018a. A repeatable geometric morphometric approach to the analysis of hand enthesal three-dimensional form. *Am. J. Phys. Anthropol.* 166, 246–260. <https://doi.org/10.1002/ajpa.23421>.

Karakostis, F.A., Hotz, G., Scherf, H., Wahl, J., Harvati, K., 2017. Occupational manual activity is reflected on the patterns among hand entheses. *Am. J. Phys. Anthropol.* 164, 30–40. <https://doi.org/10.1002/ajpa.23253>.

Karakostis, F.A., Hotz, G., Tourloukis, V., Harvati, K., 2018b. Evidence for precision grasping in Neandertal daily activities. *Sci. Adv.* 4, eaat2369. <https://doi.org/10.1126/sciadv.aat2369>.

Karakostis, F.A., Jeffery, N., Harvati, K., 2019a. Experimental proof that multivariate patterns among muscle attachments (entheses) can reflect repetitive muscle use. *Sci. Rep.* 9, 1–9. <https://doi.org/10.1038/s41598-019-53021-8>.

Karakostis, F.A., Lorenzo, C., 2016. Morphometric patterns among the 3D surface areas of human hand entheses. *Am. J. Phys. Anthropol.* 160, 694–707. <https://doi.org/10.1002/ajpa.22999>.

Karakostis, F.A., Reyes-Centeno, H., Francken, M., Hotz, G., Rademaker, K., Harvati, K., 2020. Biocultural evidence of precise manual activities in an Early Holocene individual of the high-altitude Peruvian Andes. *Am. J. Phys. Anthropol.* <https://doi.org/10.1002/ajpa.24160>.

Karakostis, F.A., Vlachodimitropoulos, D., Piagkou, M., Scherf, H., Harvati, K., Moraitis, K., 2019c. Is bone elevation in hand muscle attachments associated with biomechanical stress? A histological approach to an anthropological question. *Anat. Rec.* 302, 1093–1103. <https://doi.org/10.1002/ar.23984>.

Karakostis, F.A., Wallace, I.J., Konow, N., Harvati, K., 2019b. Experimental evidence that physical activity affects the multivariate associations among muscle attachments (entheses). *J. Exp. Biol.* 222, 213058. <https://doi.org/10.1242/jeb.213058>.

Keramopoulos, A.D., 1923. *O Apotympánismos: Symboli Archaiologiki Eis Tin Istorian Tou Poinikou Dikaiou Kai Tin Laograian*. Estia, Athens.

Klales, A.R., Ousley, S.D., Vollner, J.M., 2012. A revised method of sexing the human innominate using Phene's nonmetric traits and statistical methods. *Am. J. Phys. Anthropol.* 149, 104–114. <https://doi.org/10.1002/ajpa.22102>.

Lagia, A., 2000. *Kerameikos grabung 1999. Preliminary analysis of the human skeletal remains*. *Archäologischer Anz.* 481–483.

Larsen, C.S., 1999. *Bioarchaeology: Interpreting Behavior from the Human Skeleton*. Cambridge University Press, Cambridge.

Mariotti, V., Facchini, F., Belcastro, M.G., 2004. Enthesopathies—proposal of a standardized scoring method and applications. *Coll. Antropol.* 28, 145–159.

Mariotti, V., Facchini, F., Giovanna Belcastro, M., 2007. The study of entheses: proposal of a standardised scoring method for twenty-three entheses of the postcranial skeleton. *Coll. Antropol.* 31, 291–313.

Marzke, M.W., Toth, N., Schick, K., Reece, S., Steinberg, B., Hunt, K., Linscheid, R.L., An, K.-N., 1998. EMG study of hand muscle recruitment during hard hammer percussion manufacture of Oldowan tools. *Am. J. Phys. Anthropol.* 105, 315–332.

Merritt, C.E., 2015. The influence of body size on adult skeletal age estimation methods. *Am. J. Phys. Anthropol.* 156, 35–57. <https://doi.org/10.1002/ajpa.22626>.

Michopoulos, E., Nikita, E., Henderson, C.Y., 2017. A test of the effectiveness of the coimbra method in capturing activity-induced enthesal changes. *Int. J. Osteoarchaeol.* 27, 409–417. <https://doi.org/10.1002/oa.2564>.

Milner, G., Boldsen, J., 2016. *Transition Analysis Age Estimation Skeletal Scoring Manual*. Fordisc Version 1.02. Forensic Anthropology Center. University of Tennessee, Knoxville.

Morris, I., 2009. The eighth-century revolution. In: *A Companion to Archaic Greece*. John Wiley & Sons, Ltd, pp. 64–80. <https://doi.org/10.1002/9781444308761.ch4>.

Nicholson, N.J., 2011. *Aristocracy and Athletics in Archaic and Classical Greece*, Reissue Edition. Cambridge University Press, Cambridge.

Nikita, E., Xanthopoulou, P., Bertsatos, A., Chovalopoulou, M.-E., Hafez, I., 2019. A three-dimensional digital microscopic investigation of enthesal changes as skeletal activity markers. *Am. J. Phys. Anthropol.* 169, 704–713. <https://doi.org/10.1002/ajpa.23850>.

Noldner, L.K., Edgar, H.J.H., 2013. Technical note: 3D representation and analysis of enthesis morphology. *Am. J. Phys. Anthropol.* 152, 417–424. <https://doi.org/10.1002/ajpa.22367>.

Nolte, M., Wilczak, C., 2013. Three-dimensional surface area of the distal biceps enthesis, relationship to body size, sex, age and secular changes in a 20th century American sample. *Int. J. Osteoarchaeol.* 23, 163–174. <https://doi.org/10.1002/oa.2292>.

Osborne, R., 2009. *Greece in the Making 1200–479 BC*. Routledge, London.

Pearson, O.M., Lieberman, D.E., 2004. The aging of Wolff's “law”: ontogeny and responses to mechanical loading in cortical bone. *Am. J. Phys. Anthropol.* Suppl 39, 63–99. <https://doi.org/10.1002/ajpa.20155>.

Pelekidis, S., 1916. Excavations at Phaleron. *Archaeologikon Deltion* 2, 13–64.

Phenice, T.W., 1969. A newly developed visual method of sexing the os pubis. *Am. J. Phys. Anthropol.* 30, 297–301. <https://doi.org/10.1002/ajpa.1330300214>.

Prevedorou, E.-A., Buikstra, J.E., 2019. Bioarchaeological practice and the curation of human skeletal remains in a Greek context: the Phaleron cemetery. *Adv. Archaeol. Practice* 7, 60–67. <https://doi.org/10.1017/aap.2018.42>.

Pritchard, D.M., 2012. Sport, Democracy and War in Classical Athens. Cambridge University Press, Cambridge. <https://doi.org/10.1017/CBO9781139030519>.

Schrader, S., 2019. Activity, Diet and Social Practice: Addressing Everyday Life in Human Skeletal Remains. Bioarchaeology and Social Theory. Springer International Publishing, New York. <https://doi.org/10.1007/978-3-030-02544-1>.

Villotte, S., 2006. *Connaissances médicales actuelles, cotation des enthesopathies : nouvelle méthode*. B.M.S.A.P. 18, 65–85.

Villotte, S., Castex, D., Couallier, V., Dutour, O., Knüsel, C.J., Henry-Gambier, D., 2010. Enthesopathies as occupational stress markers: evidence from the upper limb. *Am. J. Phys. Anthropol.* 142, 224–234. <https://doi.org/10.1002/ajpa.21217>.

Villotte, S., Knüsel, C.J., 2014. “I sing of arms and of a man...”: medial epicondylitis and the sexual division of labour in prehistoric Europe. *J. Archaeol. Sci.* 43, 168–174. <https://doi.org/10.1016/j.jas.2013.12.009>.

Villotte, S., Knüsel, C.J., 2013. Understanding enthesal changes: definition and life course changes. *Int. J. Osteoarchaeol.* 23, 135–146. <https://doi.org/10.1002/oa.2289>.

Walker, P.L., 2008. Sexing skulls using discriminant function analysis of visually assessed traits. *Am. J. Phys. Anthropol.* 136, 39–50. <https://doi.org/10.1002/ajpa.20776>.

Walker, P.L., 2005. Greater sciatic notch morphology: sex, age, and population differences. *Am. J. Phys. Anthropol.* 127, 385–391. <https://doi.org/10.1002/ajpa.10422>.

Wallace, I.J., Winchester, J.M., Su, A., Boyer, D.M., Konow, N., 2017. Physical activity alters limb bone structure but not enthesal morphology. *J. Hum. Evol.* 107, 14–18. <https://doi.org/10.1016/j.jhevol.2017.02.001>.

Wilczak, C., Mariotti, V., Pany-Kucera, D., Villotte, S., Henderson, C., 2016. Training and interobserver reliability in qualitative scoring of skeletal samples. *J. Archaeol. Sci. Rep.* 11, 69–79. <https://doi.org/10.1016/j.jasrep.2016.11.033>.

Williams-Hatala, E.M., Hatala, K.G., Hiles, S., Rabey, K.N., 2016. Morphology of muscle attachment sites in the modern human hand does not reflect muscle architecture. *Sci. Rep.* 6, 1–8. <https://doi.org/10.1038/srep28353>.

Zumwalt, A., 2006. The effect of endurance exercise on the morphology of muscle attachment sites. *J. Exp. Biol.* 209, 444–454. <https://doi.org/10.1242/jeb.02028>.